C. B. Jagadeesha*

FSW between Al alloy and Mg Alloy: the comparative study

https://doi.org/10.1515/jmbm-2017-0011

Abstract: It is difficult to fusion weld Al alloy to Mg alloy, so by experimental optimization procedure (EOP) optimum parameters for FSW between Al alloy and Mg alloy were determined and experiment conducted using these parameters resulted in not only sound weld but also highest strength weld for 5 mm thickness of the alloys plates. One can arrive to optimum parameters by following the EOP in case of similar and dissimilar materials FSW, such as Al alloy and Mg alloy FSW. It has observed that tensile sample having least thickness intermetallics (IMs) layer has highest strength compared to sample with larger thickness of intermetallics layer and also it has observed that weld of lesser thickness plates have strength higher than welds of larger thickness plates. It has observed that, Vickers hardness in WN i.e. on the region containing layers of IMs is considerably higher, which leads to emerge of new type of laminated composite materials. It has observed that, it is the least thickness IMs layers in the weld are responsible for higher strength of weld not the ductility of the IMs formed owing to the insertion of intermediate material in the weld. It has found that coefficient of friction is =0.25, in case of bead on plate welding of Mg alloy.

Keywords: Al alloy; coefficient of friction; composites; friction stir welding; intermediate material; intermetallics; Mg alloy; optimization procedure; Vickers hardness.

1 Introduction

Compared to other alloys, Al alloys and Mg alloys have lower density and high specific strength. These are extensively used in automotive, aerospace and ship industries. Owing to the difference in chemical, physical and mechanical properties between components made up of Al, Mg or their alloys, the welding of dissimilar materials is generally more difficult than that of homogeneous materials. It is difficult to produce high quality Al, Mg dissimilar joint by fusion welding technique for the following reasons: the formation of brittle intermetallics (IMs) and formation of cracks. So dissimilar welding of Mg, Al and their alloys is a challenging technique to be developed.

Friction stir welding (FSW) is an innovative method developed by TWI in UK in 1991 [1]. Sound butt and lap welds have been accomplished by FSW [2]. Use of FSW to weld Al alloys [3] and Mg alloys or, to weld Al alloy to Mg alloy has increased substantially in recent years, since these are difficult to weld by fusion welding technique [4]. The side of the tool where linear velocity vector of the rotating tool is same as the welding direction vector is called advancing side (AS) and the side where both of these vectors are opposite to each other is called retreating side (RS). The front portion of the moving tool is called leading edge and the back portion of the tool is called trailing edge. Weld nugget (WN) is the core of the FSW volume and is completely dynamically recrystallized, since it is subjected to severe plastic deformation [5]. The plastic deformation is confined to WN and thermomechanically affected zone (TMAZ) only. TMAZ is not recrystallized. Heat affected zone (HAZ) is not subjected to plastic deformation and so not recrystallized but it experiences a thermal cycle.

The study by Somasekharan and Murr [6] reports that the weld zone in the welds of the Mg alloys to Al alloy 6061-T6 showed unique dissimilar weld, flow characteristics, such as complex intercalated microstructures with recrystallized lamella like shear bands rich in either Mg or Al. Sato et al. [7] report that the dissimilar weld between Al alloy 1050 and Mg alloy AZ31, had a large volume of intermetallic (IM) compound $Al_{12}Mg_{17}$ and significantly higher hardness in the weld center. Yan et al. [8] report that $Al_{12}Mg_{17}$ and Al_3Mg_2 cause the weld to crack during FSW of AZ31Mg/1060Al on the centerline of the weld. Hirano et al. [9] carried out 1050 Al alloy to AZ31B-O Mg alloy dissimilar FSW on 6 mm thickness plates and reported mechanical properties of sound weld. Zettler [10] reports that, in AZ31 Mg alloy to 6040 Al alloy FSW, the intermetallic leads to a loss of strength and ductility of the joint. Khodir et al. [11] report that, in dissimilar FSW of 2024-T3 Al alloy to AZ31 Mg alloy, the hardness value fluctuates in the WN due to formation of intermetallic compounds owing to constitutional liquation during welding.

***Corresponding author: C. B. Jagadeesha,** Department of Mechanical Engineering, Indian Institute of Science, Bangalore, Bengaluru 560012, India, Tel.: +91 9880529105, Fax: +91 80 2360 0648, e-mail: jagscb1966@gmail.com

Park et al. [12] reported FSW between 1050 and AZ31B containing large IM compound $Al_{12}Mg_{17}$ in the weld center. The formation of $Al_{12}Mg_{17}$ and Al_3Mg_2 IM compounds are inevitable in the dissimilar Al-Mg weld joints under all conditions of the welding [13]. Al-Mg IMs have high hardness and low ductility.

Friction Stir Welds having tortuous weld interfaces were reported in the dissimilar Al alloy to Mg alloy [6, 7, 14–16], dissimilar Al alloys [17–19], steel to Al [20], similar metal AZ31 Mg alloy [21] and 6061 Al alloy butt welds with pure Al marker material [22]. In dissimilar alloy welds, the geometrically complex interface might improve the strength of joint by 25–35% compared to strength of joint of metallurgical bonding alone [23].

Entire literature on FSW is based on trial and error procedure to obtain sound FSW joints. As there is no experimental optimization procedure in FSW reported in literature, here the author has made a maiden attempt to propound an experimental optimization procedure (EOP) by which one can arrive to optimum parameters to obtain not only sound similar (Al alloy or Mg alloy) or dissimilar materials (between Al alloy and Mg alloy) friction stir welds but also to obtain possible highest strength of welds. This optimization procedure at least redefines the FSW of Al alloys and Mg alloys and FSW between Al alloys and Mg alloys.

This study investigates the effect of interface offset (IO) variation on the quality and properties of friction stir welded samples and on the magnitude of thickness of IM layer in the samples and the effect of the thickness of IM layer on the tensile strength of friction stir welded tensile samples. Also this study investigates about microstructure of weld nugget of the welded samples and the hardness behavior of dynamically recrystallized materials (2024-T3 Al alloy and AZ31B Mg alloy) and their IM layer, along with the materials in WN.

In FSW of dissimilar materials (AA 6061-T6 to AZ31-H24) plates of 4 mm thickness, a third or intermediate metal has been placed between the faying edges to eliminate brittle Al, Mg IM phases or replace it with more ductile phases. Ni has been selected through the investigation of Al, Mg, Ni ternary phase diagrams showing metallic phase and ductile IM phase regions under the similar temperature of FSW. Al alloy was kept in AS and Mg alloy was kept in RS; in between the faying surfaces the Ni foil of 0.5 mm thickness and 4 mm wide were placed. The following welds were performed, (1) Dissimilar FSW of Al/Mg alloy at 800 rpm and welding speed of 35 mm/min; obtained maximum tensile strength is 95 Mpa. (2) Dissimilar FSW of Al/Mg alloy with Ni foil of thickness 0.5 mm, as intermediate metal at 800 rpm and welding speed of 35 mm/min; obtained maximum tensile strength is 115 MPa. The increase in strength of weld seems owing to formation of IM compound Ni_3Al and less formation of brittle IM compound $Al_{12}Mg_{17}$. Ni_3Al is known to be a ductile IM phase compared to $Al_{12}Mg_{17}$ [24].

Here the author has studied the effect of 0.1 mm thickness Zn foil (and Cu) and 0.1 mm (and 0.25 mm) Nickel foil as the intermediate material kept in between Al alloy and Mg alloy plates during FSW of dissimilar materials. What the author was thought that the Zn foil will dissolve partially in Al alloy and Mg alloy metals and solid solutions of Al and Zn, and Mg and Zn will replace or occupy the Al and Zn, and Mg and Zn interfaces respectively, yielding a high strength weld. But this could not happen and the technical reasons for this phenomenon are explained in this study. Woong [24] (see previous paragraph) has got higher strength equal to 115 MPa for weld with Ni foil of 0.5 mm thickness as the intermediate material compared to strength of 95 MPa for bare Al alloy to Mg alloy weld. But here in this study welds obtained with Ni foil as the intermediate material (0.1, 0.25 mm thicknesses) yielded tensile strengths of only 50, 53 MPa for 0.1 and 0.25 mm Ni foil, respectively, compared to strength of 106.86 MPa for bare Al alloy to Mg alloy weld. The reasons for the decrease in strength are explained in this study.

The thermal models that require accurate measurement of temperature during FSW need precise frictional data. Even though there is a difference between theoretical and experimental values of the coefficient of friction (μ), in FSW thermal modeling a value of $\mu = 0.4$ is assumed for calculations corresponding to various temperatures and pressures [25–28]. In many cases μ was assumed instead of actual measurements [29]. However, for the model to be akin to existing FSW conditions, one needs to know the correct value of μ. There is lack of authentic data on the variation of μ in FSW, at varying temperatures and relative velocities [30]. Frictional characteristics existing at high temperatures and pressures are still not clearly understood [31]. Thomson and Chen [32] claimed that through a theoretical approach, μ cannot be greater than 0.577; but Duffin and Bahrani [33] experimentally determined that μ is greater than 0.57 during friction welding. The findings of another experiment [34] states that μ and temperature do have a synergetic influence on each other; the value of μ in FSW condition has been found to be as high as 1.2–1.4 at 400°C to 450°C. The temperature and contact pressure in FSW appear to be beyond the seizure limit [34]. Therefore, there seems to be an exigency to make a systematic approach to determine the value of μ for in-depth studies on some aspects of FSW. Here μ (=0.25) has determined

from pragmatic approach, compared to μ determined from non pragmatic approach [34].

2 Experimental

Indigenously developed computer controlled FSW machine (BiSS Bangalore) was used for all FSW experiments. The base materials used were 2024-T3 Al alloy and AZ31B-O Mg alloy. Composition of 2024-T3 Al alloy: 4.3–4.5%, copper; 0.5–0.6%, manganese; 1.3–1.5%, magnesium and less than a 0.5% of silicon, zinc, nickel, chromium, lead and bismuth. This has tensile strength = 400–427 MPa, yield tensile strength = 269–275 MPa, elongation = 10–15%, Young's modulus = 73 GPa, melting point = 502–638°. Composition of AZ31B-O Mg alloy: 2.5–3.5%, Aluminum; 0.7–1.3%, zinc and 0.20–1.0%, manganese. This has tensile strength = 240 MPa, yield tensile strength = 140 MPa, elongation = 10%, Young's modulus = 45 GPa, melting point = 605–630°. The size of Al alloy and Mg alloy plates: 250 mm × 80 mm × 5 mm. Where, 5 mm is the thickness (t) of plates.

EOP in brief has illustrated as follows.

1. Choose the tool material by comparing with the materials of the workpieces [35] (here HDS tool was chose for FSW of Al alloy to Mg alloy material workpieces).
2. Choose the geometry of the tool by comparing with the thickness (t) of workpiece materials, preferably as suggested by Prado and Murr [36] (here pin length = 4.7 mm, pin top diameter = 6 mm, bottom diameter = 4 mm, shoulder diameter = 15 mm with rounded pin end was chose).
3. Take shoulder diameter = 3 × t (here t = 5 mm) for Al alloy to Mg alloy weld. Choose pin length of 4.7 or 4.67 mm, which is 0.3 mm less than t; set the plunge depth (PD) of tool = 4.9 mm, leaving 0.1 mm distance between tool pin tip and bottom surface of workpiece and tool tilt angle (θ) = 2°.
4. Do the bead on plate welding (or FSP) on any one plate material (here Mg alloy). Select a range of speed (here 300 to 800) and a high traverse speed (V) = 100 mm/min. After welding, if a through hole obtained along the length of weld, then keeping all other parameters same decrease (step by step) V until no through hole obtained. Here a good weld was resulted for bead on plate welding (or FSP) of Mg alloy plate for V = 60 mm/min and 340 rpm (Figure 1).
5. The author did the dissimilar weld by keeping harder material (here Al alloy) in AS with the above same tool by setting 300 to 1000 rpm, V = 50 mm/min and zero IO (Figure 2) and then he selected rpm range from 300 to 400 rpm corresponding to not cracked length of the weld; he did weld (Figure 3) with other parameters repeated and then he obtained the metallographic samples to determine the rpm {here 305 rpm (Figure 4)} at which sound weld was resulted.
6. Next the author did IO variation weld at 300 rpm (say Exp.1) repeating the same parameters (Figure 5) and found the region (on either side of zero IO) in which sound weld occurred by observing tensile and microstructure samples cut from the weld coupon.

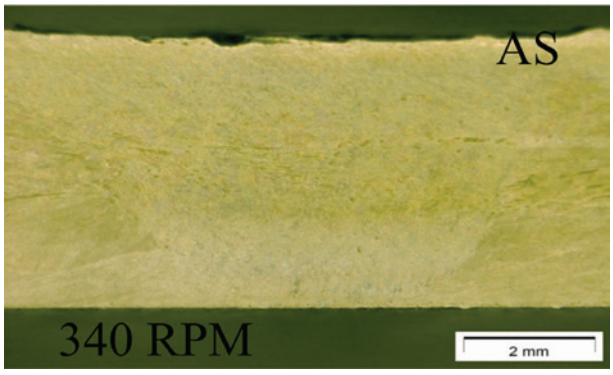

Figure 1: Optical macrograph of bead on plate welded AZ31B-O Mg alloy plate cross section sample at 340 rpm.

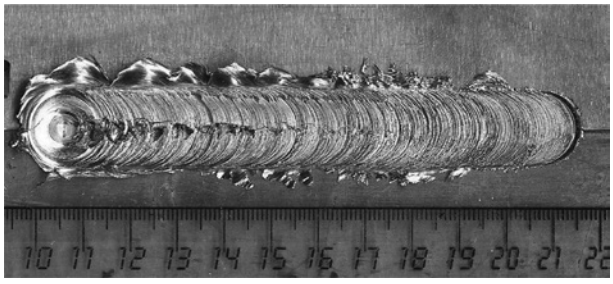

Figure 2: Weld coupon obtained at parameters, 300–1000 rpm, 50 mm/min welding speed, zero IO, from FSW between 2024-T3 Al alloy and AZ31B-O Mg alloy plates; tool withdrawn at about 700 rpm.

Steps 1 to 4 can be used for any FSP. One can compare this procedure for FSP with that of Naresh [37] (see below) and can realize the simplicity and feasibility of the procedure.

Naresh [37] approach for Optimization Procedure in FSP is as follows (as it is in the paper [37]):

1. Varying plunge depth experiment

Tool rotation rate and traverse speed were kept constant at 500 rpm and 25 mm/min respectively. Plunge depth was varied from 5 mm to 5.8 mm for a processing distance of 200 mm and a tool pin length of 5.4 mm. For each 20 mm

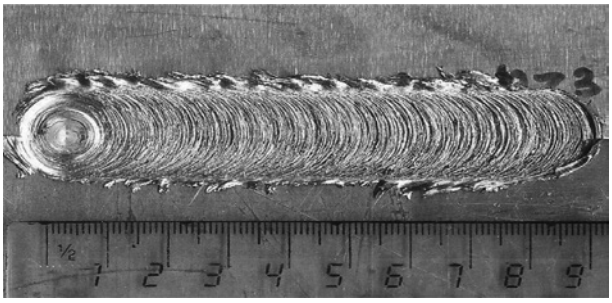

Figure 3: Weld coupon obtained at parameters, 300 to 400 rpm, 50 mm/min welding speed, zero IO, from FSW between 2024-T3 Al alloy and AZ31B-O Mg alloy plates.

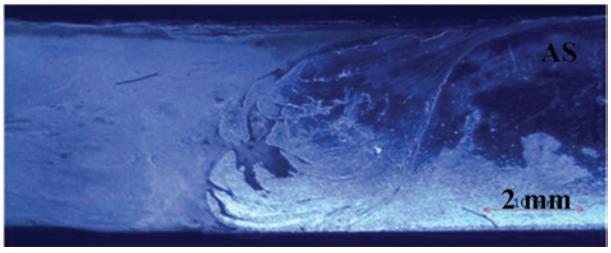

Figure 4: Photomicrograph of cross sectioned sample at 305 rpm and 50 mm/min welding speed, obtained from weld coupon of Figure 3.

of FSP region, a tensile and micro structural specimen was taken. Optimum plunge depth was selected by correlating the ultimate tensile strength and observing the macrograph taken for each sample.

2. Varying rpm experiment

With the obtained optimum plunge depth of 5.63 mm from the above set of varying plunge depth experiments and keeping the same constant traverse speed, tool rotational rate was varied from 200 to 1600 rpm. This was done in two steps – in the first step rpm was varied from 200 to 900 and in the next from 900 to 1600.

3. Varying traverse speed exp.

With the obtained optimum plunge depth and rotational speed from above two experiments traverse speed was varied from 10 to 170 mm/min. here too the experiment was done in two steps – in first stage by varying traverse speed from 10 to 90 mm/min, and in the next by varying from 90 to 170 mm/min.

4. Optimum FSP experiment with the optimum processing parameters

The optimum process parameters were selected from the above experiments and an optimum FSP has been done.

Figure 5: Surface morphology of the FSW coupon of Al alloy to Mg alloy, obtained by interface offset varying welding with parameters: rotational speed = 300 rev min^{-1}, welding speed = 50 mm min^{-1}.

The following questions have arisen about this approach.

1. Why should one has to take 500 rpm and V = 25 mm/min as starting values? Why cannot one take values other than these? What is the justification behind choosing these values? rpm and V have synergistic effect on each other.
2. So there is no justification behind choosing these (above) values and also choosing constant V = 25 mm/min in varying rpm experiment.
3. One can choose other arbitrary values by his guess; yes there is equal probability of choosing other values randomly; or can one choose any guessed value?
4. Why V = 25 mm/min, preferably? Why not any other value? There is possibility of choosing different V's by different persons, which one is more suitable?
5. It is certain that, if one chooses other values for the parameters other than chosen by another person, one definitely ends up to the optimum parameters values other than the optimum values got by Naresh [37]. Definitely this is possible, why not? Then how do one decide which are optimum parameters? Then there will be infinite combinations of optimum parameters. But all, so called optimum parameters cannot yield sound FSP, only one combination of parameters give the best sound FSP, but those parameters cannot be reached by this approach; so FSP obtained by parameters other than best must be defective. Defects may be visible or not visible to eyes, they may be minute or microscopic. So one can conclude that, first of all Naresh [37] has not obtained optimum parameters for his FSP and his approach will not result in optimum parameters, yielding sound FSP/FSW.

The EOP here in this paper is a very simple, systematic, logical, and effective procedure yielding or arriving quickly to the optimized parameters in FSW/FSP. The FSW produced between Al alloy and Mg alloy here in this paper is the best evidence for the feasibility of the EOP. This EOP is especially suited to FSW/FSP of precipitable Al alloys, since HAZ (becomes weaker as the rpm increases and so the temperature of weld volume also increases) will be

Figure 6: Weld coupon obtained with Zn as intermediate metal; at the mid region of welded plate there is no longitudinal crack indicating good weld there. Most of the microstructure samples of this coupon were broken during cutting.

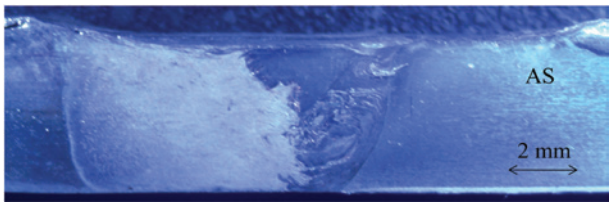

Figure 7: Macrograph with Cu as intermediate metal with intercalated Cu layers in WN.

little affected during and after FSW. Overaging of HAZ is prevented owing to use of low rpm and medium V during FSW by following the EOP reported here.

Exp. 2. Interface offset (IO) varied FSW (IO of 2 mm on AS and 2 mm on RS from zero IO or leading edge) between 2024-T3 Al alloy and AZ31B-O Mg alloy of 5 mm thickness plates was performed at 305 rpm and 50 mm/min with insertion of 0.1 mm thickness Zn foil as the intermediate material (Figure 6). Here good weld obtained but tensile strength of the weld was almost zero MPa. All tensile samples were failed near to zero MPa and most of the samples of microstructures were broken during cutting.

Exp. 3. Interface offset (IO) varied FSW (IO of 2 mm on AS and 2 mm on RS from zero IO or leading edge) between 2024-T3 Al alloy and AZ31B-O Mg alloy of 5 mm thickness plates was performed at 305 rpm and 50 mm/min with insertion of 0.1 mm thickness Cu foil as the intermediate material (Figure 7). Here good weld obtained but tensile strength of the weld was almost zero MPa. All tensile samples were failed near to zero MPA and most of the samples of microstructures were broken during cutting.

Exp. 4 and 5. Interface offset (IO) varied FSWs (IO of 2 mm on AS and 2 mm on RS from zero IO or leading edge) between A 2024-T3 Al alloy and AZ31B-O Mg alloy of 5 mm thickness plates was performed at 305 rpm and 50 mm/min with insertion of 0.1 mm and 0.25 mm thickness Ni foils separately as the intermediate materials. Here good welds were obtained with maximum tensile strengths of 53 MPa and 50 MPa for 0.25 and 0.1 mm Ni foils respectively. The corresponding microstructures are similar to Figure 7.

Experiment conducted by [34] can be enumerated as follows: the cylindrical pin in contact with the flat base material surface is carefully rotated around its axis using a motor. The base material is either fixed or held on to the lever assembly, which is kept on a thrust bearing. The average μ values were calculated from the measured tangential load and applied axial load. This experimental set up no way resembles actual FSW process. On the other hand in the actual FSW process, outer surface of weld volume is a 3D surface of the shape of inverted bell (where the main shearing of plasticized material from TMAZ zone, considered occurring) instead of small flat surface as taken in above said experiment. In actual FSW what is happening is as explained above. Here these points are considered and μ is determined from actual FSW experimental conditions rather than determining μ from non pragmatic experimentation as reported in [34]. This work reports about equivalent coefficient of friction ($\mu_s = 0.25$) in bead on plate welding of AZ31B-O Mg alloy material.

3 Results and discussion

3.1 Experimental optimization procedure (EOP)

The hardness of work pieces determine what type of the tool material [35] ought to be. First of all proper tool material (here HDS) was chosen for a particular workpiece materials (here AA 2024-T3 and AZ31B-O) combination. Also the tool dimensions are considered by the thickness of the workpiece only. The tool was chosen according to the self optimized tool geometry suggested by Prado and Murr [36].

Pin of length 4.7 mm, top pin diameter of 6 mm and bottom pin diameter of 4 mm, resulting in mean diameter at 5 mm and at bottom pin has rounded end; diameter of shoulder = 20 mm, θ = 2°. Plunge depth (PD) of tool = 4.9 mm has set, leaving 0.1 mm (or a maximum of 0.15 mm since a low rpm of 300 rpm has employed during FSW) distance between tool pin tip and bottom surface of the workpiece during FSW. By this there will be no, not jointed interface between the two plates, below the tip of pin during and after welding. 200 rpm is too low rpm and 800 rpm is too high, and also V = 120 mm/min is quite high for Mg alloy FSW, so, for a bead on plate welding of AZ31B-O plate the following parameters chosen by educated guess: rpm = 300 to 800; θ = 2°; PD = 4.9; traverse speed (V) = 100 mm/min, but this did not yield the good surface morphology or surface look of the weld. Keeping everything same and using a tool with shoulder diameter

(D) = 15 mm equal to 3 times the thickness of workpiece, 5 mm, the weld was performed yielding a good surface morphology. D will be > 15 mm for still harder workpiece materials. Malarvizhi and Balasubramanian [38] claims that, in FSW of Al alloy to Mg alloy the ratio between shoulder diameter and thickness of workpiece should be 3.5 to get good weld, but here the author used the ratio, 3 to get good weld between Al alloy and Mg alloy. For all further FSW experiments reported here, the ratio 3 was used. For this weld (D = 15 mm) a through hole inside the weld volume and along the length of the weld was obtained, which was ascribed to high V, and this was owing to lack of consolidation or forging action on the workpiece material in the weld volume. PD is already at its maximum and it no longer being increased further to eliminate through hole.

The welding speed contributes to the heat generation lesser than the heat generation by the chosen rotational speed. But in contributing to the forging action on weld, the welding speed comes next to the axial load. Interestingly, higher the welding speed decreases the forging action, and lower the welding speed increases the forging action. As the welding speed decreases, both the heat input to the material as well as the forging action being exercised on the material within weld volume increases. Because the welding speed is less, the tool spends more time at the region over the plate surface where it is rotating resulting in well consolidated weld. Forging action on the weld volume for lesser welding speed occurs for more time per mm of forward motion of FSW tool than the forging action for higher welding speed. This concept confutes the idea, i.e. welding speed does not have much effect on the quality of the weld.

Keeping all parameters and other things same as in previous experiment, welding was done for V = 80 mm/min, again a smaller through hole inside the weld volume and along the length of the weld was obtained. Next another weld performed for V = 60 mm/min keeping other parameters same and taking the same previous tool; a good weld was obtained at 340 rpm (Figure 1).

As the rotational speed increased, the flow stress of the material decreases and also the forging action increases owing to reduced welding speed of 60 mm/min. Consequently for this experiment the defects altogether disappeared at 340 rpm resulting in sound weld. Pressure on weld volume depends on plunge depth (PD) of tool and traverse speed, since both are constant and rpm increase from a lower value to higher value, plasticization of materials in weld volume increases from low at low rpm to high at higher rpm. At a certain rpm (340 rpm in above paragraph) and at corresponding plasticization of material, material fills each and every corner in the weld volume resulting in well consolidated and sound weld. The parameters at this state can be called optimized parameters and pressure in the weld volume is optimum pressure. After optimum rpm material plasticizes to more extent and flash results owing to more softened material escaping out of the weld volume resulting in defective weld.

Sound weld is directly dependent on flow stress of the WP material, which in turn depends on rpm of FSW tool. Pressure created by FSW tool shoulder on the material in the weld volume, which (pressure) in turn in turn depends on traverse speed of the tool. Low traverse speed (40 to 60 mm/min) gives highest pressure on the weld volume or highest forging action on the material in the weld volume thus consolidating the material in the weld volume yielding sound weld. Flow stress of material depends on rpm (and so temperature) and traverse speed (V); higher the rpm of the tool, higher the plastic deformation of the material in the weld volume and so higher is the temperature in the weld volume. Lower the V higher the rpm, per mm motion of the tool so higher the work done and higher the heat generation owing to longer duration of plastic deformation of the material below the shoulder of the tool and material adjacent to FSW tool pin. Duration in min ($=T_{pr}$) in which pressure is acting on the material in the weld volume per mm motion of the tool = 1/V in min/mm. Optimum pressure giving sound weld occurs when V is low for particular WP material and tool material combination.

Pressure on the weld volume is more for less traverse speed than higher traverse speed, because tool stays for more time per mm of traverse of the tool on the weld volume at less traverse speed. Let us say we have got a sound weld at high rpm and high traverse speed. The pressure in this case is lesser compared to pressure at low traverse speed and low rpm as said in previous paragraph, and also this pressure action takes place for a lesser duration owing to higher traverse speed than the pressure action in the case of low rpm and low traverse speed. In the case of low rpm and low traverse speed, owing to high pressure action for longer duration and lesser temperature rise in weld volume owing to low rpm, there occurs optimum diffusion between the plasticized materials in weld volume compared to high rpm, high V, resulting in higher strength weld. For lower traverse speed, pressure owing to PD of tool, acts more time per mm of movement of tool, on weld volume than that for higher traverse speed.

During the dissimilar FSW, 2024-T3 Al alloy and AZ31B-O Mg alloy plates were kept in AS and RS of FSW tool respectively. FSW Tool material was HDS and tool

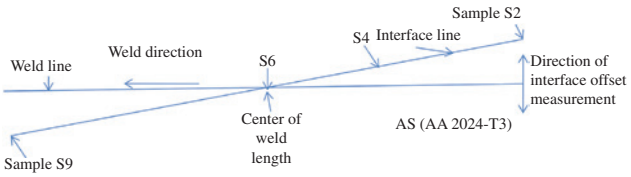

Figure 8: Outline for dissimilar material (between 2024-T3 Al alloy and AZ31B-O Mg alloy) varying interface offset welding (image shown in Figure 5).

had threaded pin with top diameter 6 mm, bottom diameter 4 mm, tool shoulder diameter 15 mm and pin length = 4.67 mm (this tool was also used for all the following welds). Rotational speed varied from 300 to 1000 rpm, welding speed = 50 mm/min, tool plunge depth = 4.88 mm. As a significant step, the author devised to set zero interface offset (IO). For zero IO, both the interface of plates and tool center line lie on same plane or line. During these parameters welding, welding was intercepted in between and weld tool was withdrawn since through crack had occurred after 400 rpm (Figure 2), owing to quick formation of brittle Al-Mg intermetallics (IMs) at higher rpm and so at higher temperatures. Then keeping all other parameters constant, a weld was carried out by varying rotational speed from 300 to 400 rpm (Figure 3). After welding, metallographic samples were prepared from the weld coupon (Figure 3). Sound weld was obtained at 305 rpm (Figure 4).

For the given set of parameters, there exists a window of interface position, in relation to the tool (0.5–1.5 mm away from the tool center) in the AS which gives the optimal strength and ductility without a joint line remnant (JLR), for similar workpieces thickness of 5 mm and bottom tool pin diameter of 4 mm. Similar study can be used to find out optimum location to position the initial interface in dissimilar welds; however the safe range is expected to change based on the tool, base metal properties and the processing parameters [39].

Varying interface weld performed for AA 2024 and AZ31B-O dissimilar material combination for the following parameters; rotational speed = 300 rpm, starting interface offset is 2 mm in RS and ending interface offset is 2 mm in AS, welding speed = 50 mm/min, plunge depth = 4.88 mm, weld length = 200 mm and tool tilt angle 2°. After welding, metallographic samples and tensile samples were extracted alternatively from weld coupon (Figure 5). In metallographic samples, Al alloy side was etched by using Kellers Reagent (1 ml HF + 1.5 ml HCl + 2.5 ml HNO_3 + 95 ml distilled water) for 30–50 s and Mg alloy side was etched by solution (14 ml out of "2g picric acid + 20 ml ethanol" + 2 ml acetic acid + 2 ml water) for 5 s [13].

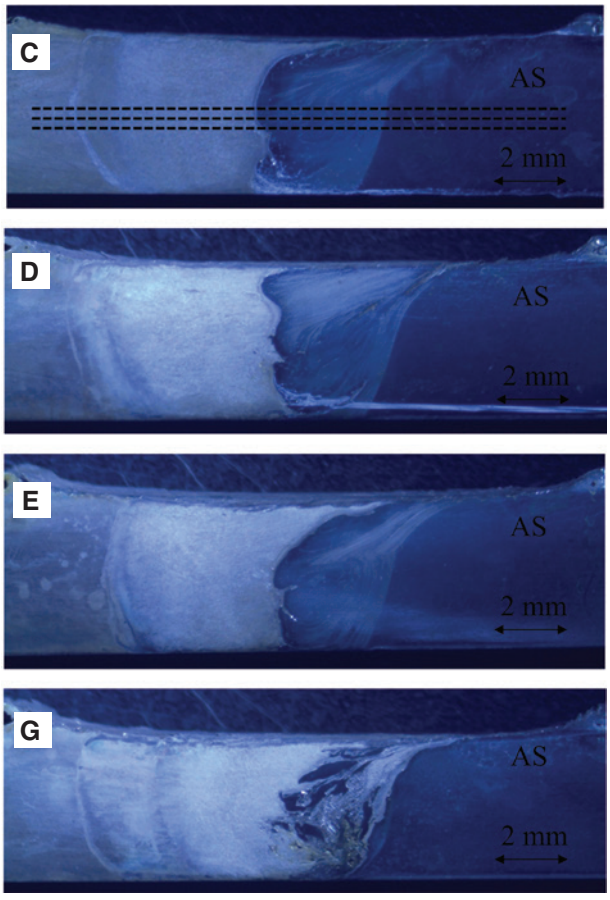

Figure 9: Cross-sectional macrostructures of the joint samples S2 or (a) to S9 or (h), cut from interface varied weld coupon shown in Figure 5.
(C) Cross-sectional macrostructure of the joint sample S4. (D) Cross-sectional macrostructure of the joint sample S5. (E) Cross-sectional macrostructure of the joint sample S6. (G) Cross-sectional macrostructure of the joint sample S8. Similar defective macrostructures are obtained for samples S2, S3, S7, and S9.

3.2 Macrostructure of joints

Exact position of the interface required for good weld for particular combination of materials can be determined by performing varying interface offset position FSW experiment for optimized parameters (tool centerline positioned, $\pm R_b$ mm on either side of interface line; R_b being the bottom radius of tool pin, here $R_b = 2$ mm) and then finding out the position range for best weld [39]. Figure 8 shows outline for dissimilar material varying IO welding. Above (Figure 9) are the macro images of samples cut along the weld line shown in Figure 5 and Table 1, for interface offset varying weld between 2024-T3 Al alloy and AZ31B-O Mg alloy plates performed at a rotation speed of 300 rev min^{-1} and 50 mm min^{-1}.

Table 1: Interface offset positions for various samples cut along the weld line shown in Figures 5 and 8.

Samples shown in Figure 9	Interface offset from weld line in mm	
	In (RS)	In AS
S2 or (a)	1.56	
S3 or (b)	1.16	
S4 or (c)	0.76	
S5 or (d)	0.36	
S6 or (e)		0.04
S7 or (f)		0.48
S8 or (g)		0.84
S9 or (h)		1.24

Samples S1 and S10 were broken during cutting.

Figure 9 shows macroscopic images of the cross sections of the dissimilar joints for IO varying weld. Joint of samples S4 or (C), S5 or (D) and S6 or (E) are free from defects while joint line remnant (JLR) was observed in middle region for these samples. The reason for vertical but little curved JLR or IM layer at the central portion of weld volume is FSW was carried out at a lower rotational speed (300 rev min^{-1}). The type of WN region structure and the IM distribution is directly dependant on rotational speed employed. The quality of the weld is assessed through various tests. In further sections the characterization of welds, by analyzing many aspects of properties of welds, is made.

3.3 Microstructure of joints

Equiaxed grains in Mg side of WN with much smaller size compared to those in Mg base metal and small lamellar like grains in Al side of WN compared to large lamellar like grains in Al base metal (Figure 10) are on left and right sides of the central IM layer respectively (Figure 9C–E). In Figure 9C–E there is a continuous and very thin IM layer as visible in Figure 11A–C. Less thickness IM layer formed since diffusion is very less due to low strain rate owing to low rotation speed and so low temperature at the WN region; The IM layer mainly contains IM compound $Al_{12}Mg_{17}$ along with Al_3Mg_2; since the $Al_{12}Mg_{17}$ is formed at low temperature [11]. Yashan et al. [40] suggests in a study on FSW of 1100 Al and type 316 stainless steel that

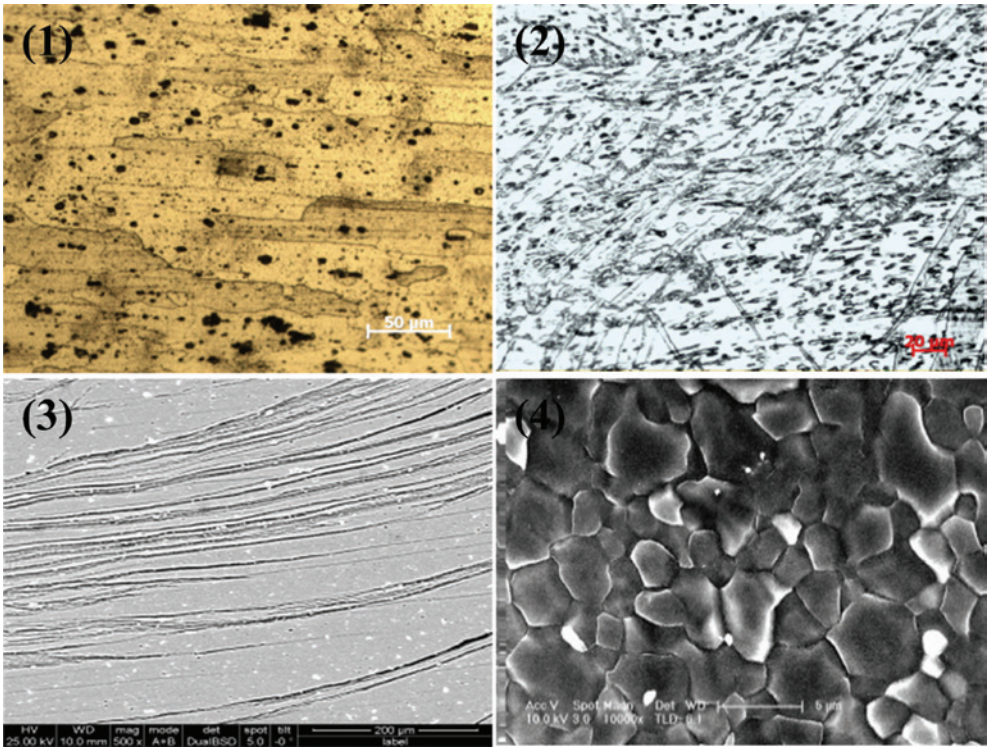

Figure 10: (1) Photomicrograph of Al 2024-T3 base metal. Average grain size = 160 × 32 µm (2) Photomicrograph of AZ31B-O base metal. Average grain size = 50 × 12 µm (3) SEM image of Al 2024-T3 side of WN. Average grain size = 60 × 22 µm (4) SEM image of AZ31B-O side of WN. Average grain size = 2.2 µm. Photomicrographs 1 and 2 are obtained from samples, which were used to obtain SEM images 3 and 4 respectively.

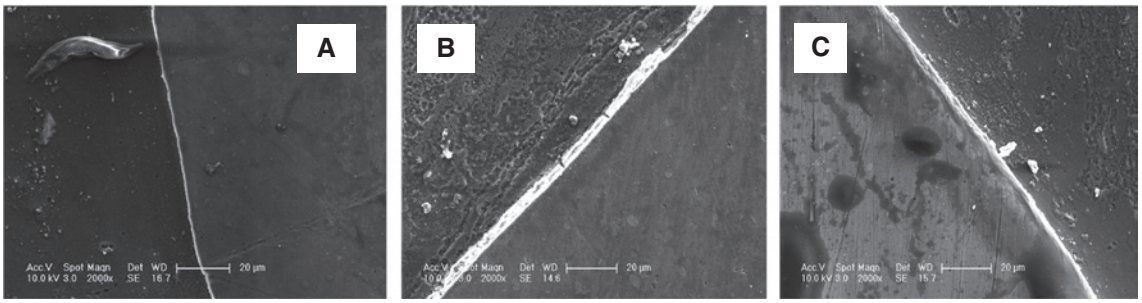

Figure 11: SEM images taken at same magnification showing IM thickness "t" at central WN region of samples S4, S5 and S6. (A) For sample S4 with IO = 0.76 mm in RS, average t = 1.2 μm. (B) For sample S5 with IO = 0.30 mm in RS, average t = 3 μm. (C) For sample S6 with IO = 0.04 mm in AS, average t = 2.5 μm.

the diffusion is enhanced during plastic deformation with a high strain rate. Similar to micrographs of Figure 11, the author has taken other SEM images in each sample at the other three regions in the same sample WN, having almost same IM thickness.

3.4 X-ray diffraction (XRD) analysis

Figure 12 contains some peaks obtained from XRD analysis on sample S6 (Figure 9E). Large peaks of IM compound $Al_{12}Mg_{17}$ are detected. XRD patterns confirm that the presence of IM compounds $Al_{12}Mg_{17}$ and Al_3Mg_2 in the IM layer in WN. The IM formation of both types ($Al_{12}Mg_{17}$ and Al_3Mg_2) of compounds was reported in the Al-Mg laser welds [41] and FSW lap [42] and butt welds [43].

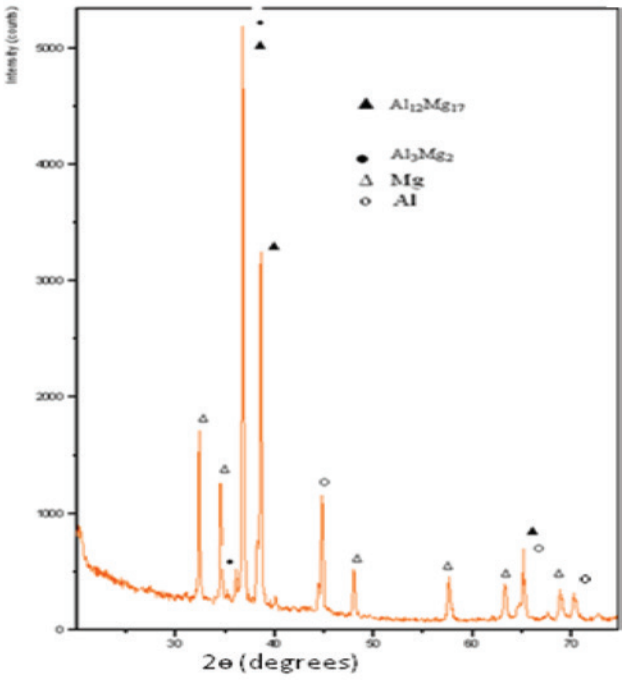

Figure 12: X-ray diffraction pattern of the sample S6 (Figure 9E).

3.5 Tensile strength analysis

The tensile samples conform to ASTM standards. Dimensions of, one of the tensile samples is shown in Figure 13A. A nano UTM (BiSS Bangalore) with maximum capacity of 15 kN was used for tensile testing of the samples at a strain rate of 10^{-3} s^{-1}. Tensile strength of each sample recorded and plotted as shown in Figure 13B. In Figure 13B, positive values of IO positions are towards RS from the position of zero offset, negative values of IO positions are towards AS from the position of zero offset. Zero IO coincides with leading edge.

The reason for maximum tensile strength at D (Figure 13B) is, at that IO of D, IM layer of least thickness forms along with good bonding between IM layer and the recrystallized alloy materials on either side of IM layer. Sample S4 (Figure 11A) has IO = 0.76 mm in RS and has least IM thickness, sample D (Figure 13B) has IO = 0.66 mm in RS, which is near to S4, and so D also has almost same least IM thickness. On the same line one can conclude that sample C has IM layer of thickness as that of S5 and sample B has IM layer of thickness as that of S6. When the interface of the two alloy materials lies in the range of IO from B to D (Figure 13B), the interface experiences higher compressive strain and strain rates as well as medium (about π/2 rad) shear strain and shear strain rates owing to forward moving and rotating tool, because the extruded material by the forward moving tool is in crescent shaped cross section with wider top and thicker at top middle (i.e. at zero IO) and narrow bottom [44, 45]. So plastic deformation of the alloy materials is higher and also diffusion between alloy materials in weld volume is higher if the interface lies in the region between B to D, especially these are higher at region C. So sample

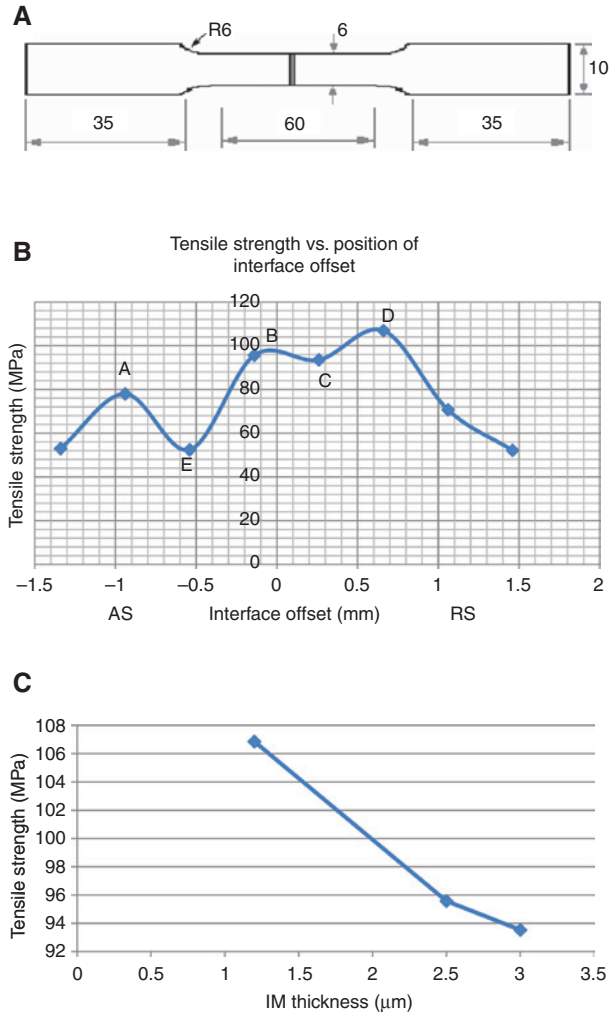

Figure 13: (A) Dimension of tensile sample. (B) Tensile strength of tensile samples at various interface offset positions. (C) Plot of tensile strength versus IM thickness.

C has larger IM thickness (Figure 11B) and also, it has comparatively lesser tensile strength than B and D. The reason for highest tensile strength at D, having least IM thickness is that strain energy increases as the volume of IM layer decreases [46]; volume of IM layer is least for tensile sample D having least IM thickness. As the strain energy is more, corresponding tensile strength is highest for tensile sample at D. Tensile strength decreases as the IM layer thickness increases in WN (Figure 13C). Highest tensile strength of 106.86 MPa was obtained for the tensile specimen with IMs thickness 1.2 μm and tensile strength of 93.5 MPa was obtained for tensile specimen with IMs thickness 3 μm.

Similar results were obtained by Venkateswaran and Reynolds [13]. Venkateswaran and Reynolds [13] have plotted the variation of the tensile strength as a function of the maximum IM thickness by taking many points. Their plot indicates that the tensile strength of the weld joint increases as the maximum thickness of the IM layer at the interface is decreased. They relate this higher bond strength for the lower IM thickness, to lower defect content in a smaller volume of IM. The reasoning by author, for highest tensile strength of D equal to 106.86 MPa (Figure 13B), with minimum IM layer thickness is already explained in previous paragraph.

Apart from the macro pictures (Figure 9) showing sound weld at 0.36 mm, 0.76 mm offsets in RS and at 0.04 mm offset in AS, there is good tensile strength, in turn sound weld (Figure 13B) between 0.3 mm (in AS) and 0.9 mm (in RS); this range of length = 0.9 + 0.3 = 1.2 mm. During FSW, keep the interface at 0.3 mm in RS of the tool so that the tool can be constrained to move along this 0.3 mm interface offset line and can sway around this line by about 0.6 mm on either side.

The maximum tensile strength and the corresponding maximum elongation of the dissimilar welds are 106.86 MPa and 1.33% respectively. Owing to the formation of brittle IMs layer and concomitant decrease in the strength of weld, the FSW joint efficiency is 44.52% (=106.86/240); the baseline tensile strength being the tensile strength of AZ31B-O Mg alloy, equal to 240 MPa.

3.6 Fractographs of tensile fracture surfaces

Diagnosis made for the fractures in tensile sample and it follows. The tensile failure of the weld joints occurred only by fracture along the central continuous vertical but slightly curved IM layer. It can be categorically stated that all the weld joints failed along the IM layer during tensile testing owing to the minimum cross section of the joint along weld center line and brittle nature of IMs, which are present in the minimum cross section. Backward tilted tool gives rise to minimum cross section of the joint along the weld center line. Figure 14 shows the cross section of an Al alloy and Mg alloy weld joint's, tensile fractured sample at B in Figure 13b. Figure 15 shows the SEM fractographs of the Al alloy side of the fractured sample at B in Figure 13b. The failure of the welded joint samples occurred through the very narrow IM layer leaving the IM compounds on both the Al and Mg sides of the fracture surfaces.

The transgranular cracking occurs in the brittle IM phases and the step like features appearing similar to cleavage facets (Figure 15). Figure 15 shows the SEM fracture morphology observed from the normal direction to the fracture surface on AS i.e. 2024-T3 Al alloy side. Cleavage like feature can be observed in the fracture surface,

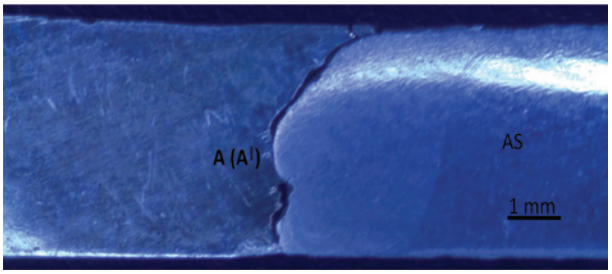

Figure 14: Tensile Fractured Sample after the tensile test.

revealing that the dissimilar weld failed altogether through brittle fracture mode.

3.7 Hardness

The micro hardness profile of one of the samples (S5) is shown in Figure 16. Future-Tech micro hardness tester FM-800 was used for indentations. The micro hardness measurements were recorded across the weld nugget at middle depth along 3 dashed black lines shown in sample 4 (Figure 9C), on the transverse cross section of the welded plate normal to the welding direction. For sample S5 Vickers hardness (Hv) values versus distance along the cross section of the sample have been plotted (Figure 16). Each plotted point on the plot is the average of 3 readings (but on IM layer 4 readings) taken along on 3 parallel lines separated by 0.25 mm. The average Vickers hardness on the IM layer in S5 is 116.18 Hv, which is the maximum of all hardness values taken on IM layers only, on each sample. Similar measurements were recorded for samples S4 and S6 and are not shown in Figure 16; but the readings were almost same with a little variation similar to variations of readings in sample S5, except the readings on IM layer. For S4 the average Hv value on IM layer is 86.20 Hv and the same for S6 is 98.67 Hv. As shown in Figure 16, the hardness value fluctuates in the WN owing to dynamic recrystallization and formation of brittle IM compounds. The tensile fracture was brittle type, and its position was located at the mid position of IM layer.

Since the thickness of IM layer is high in S5 than S4 and S6 the hardness is highest (116.18 Hv) on the IM layer of S5 and next highest (98.67 Hv) on IM layer of S6 and next highest (86.20 Hv) on IM layer of S4. Hardness is greater for S5 (with high IM thickness 3 μm) compared to S6 and S4 because there is more volume fraction of IM material in S5 with IM layer thickness of 3 μm, which participates in resisting the indentation. This observation is contrary to that of tensile strengths of samples shown in Figure 13b. It has known that $(t)_{S5} > (t)_{S6} > (t)_{S4}$, where 't' is the IM layer thickness; let "h" be the Vickers hardness on the IM layer for samples S4, S5, S6 then $(h)_{S5} > (h)_{S6} > (h)_{S4}$ so as the IM thickness increased the resistance to indentation increased and so hardness increased. The author has the images of hardness indentations; owing to shortage of space they have not been put.

For solid–solid transformations, there may be volume changes attendant to the formation of new phases. These changes may lead to the introduction of microscopic strains [47]. Crystal structures other than fcc or hcp have more volume per unit mass of substance, or crystal structures other than fcc or hcp have packing factor less than that of fcc; the IM layer has more volume than the parent materials which were in the place of IM layer, thus introducing microscopic stresses and strains in the material system (Al + IM + Mg). Higher the thickness of IM layers higher the compressive stresses in turn higher hardness value (here 116.18 Hv for highest IM thickness of 3 μm in S5). Higher compressive stresses owing to higher thickness of IM layer develop high shearing or sliding

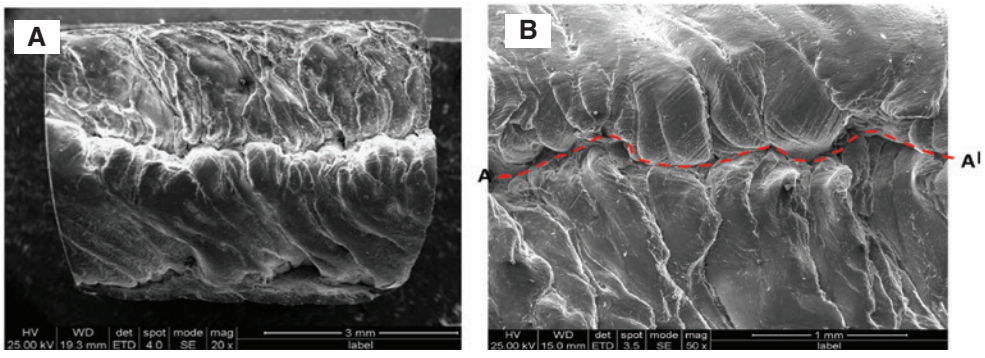

Figure 15: SEM fractographs images of tensile fracture surface (Al alloy side).
Fractograph (B) indicating the wavy line (red color) through which initiation of fracture occurred, see also Figure 14. (A) Al alloy side fractograph. (B) Enlarged (A).

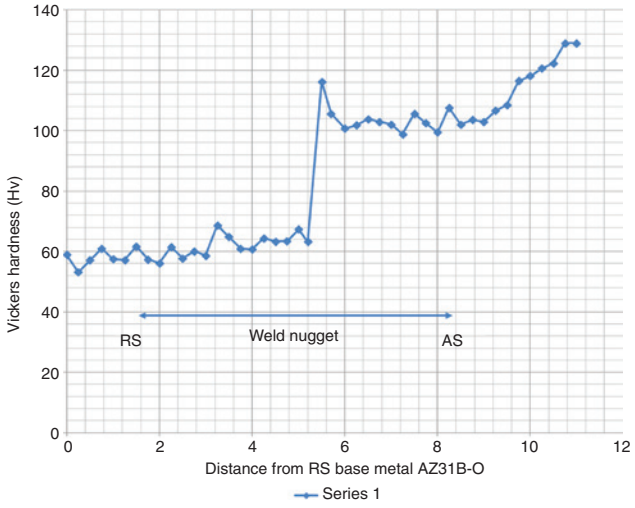

Figure 16: Vickers hardness plots of sample S5 obtained by micro indentation.

resistance between layers of materials Al, IM, Mg, for slip between layers (similar to frictional force proportional to normal force) during indentation. If a single atomic layer in case of edge dislocation develops compressive stresses, so definitely IM layer develops considerable compressive stresses and strains in it as well as in adjacent Al, Mg materials.

If one takes group of plates consisting of Al and Mg materials alternatively placed on each other and if one subjects the surface of the group of alternate plates to controlled heating or heat treatment then there occurs formation of IM layers in between Al and Mg materials at the interfaces of Al and Mg materials. As reported here hardness of Al, IM, Mg layers together directly proportional to thickness of IM layer, i.e. higher the thickness higher the hardness of system of materials. This type of material system exhibiting high hardness gives rise to new type of laminated composites. One has to do experimentation regarding this to get optimized parameters such as thickness of Al, Mg plates, heat treatment temperature and duration to which surface of plates have to be subjected to get the optimum thickness of IM layer etc. to get highest hardness of the material system.

3.8 Analysis of welds

K. Kumar in his PhD thesis, synopsis, writes "In order to obtain FSW welds with maximum joint efficiency, the welding temperature should not exceed the "softening temperature" of the base metal. If the weld formation temperature is less than the base metal softening temperature, the weld can be made with 100% joint efficiency. In order to optimize the FSW parameters, which gives defect free weld with lowest possible temperature an instrumented programmable FSW machine is to be designed and developed". Here in this work (this paper) by the author, welds were obtained at lowest rpm, resulting in less temperature rise in weld volume, which is less than the base metals softening temperature.

As the thickness of plates decrease and so cross sectional area decreases, the volume of the IMs material in weld volume decreases; so tensile strength of lesser thickness FSW plate is higher than tensile strength of higher thickness FSW plate. This can be seen in the Table 2, where strength of FSW increases as the thickness of plates decreased. On the similar grounds welds obtained at low rpm having lesser IMs thickness capable to withstand higher stresses since they have lower volume of IMs material than that of the welds obtained at higher rpm having higher IMs thickness layers (owing to increased diffusion in weld volume) and so having higher volume of IMs.

Author should have got lesser tensile strength of the dissimilar weld for 5 mm thickness plates than tensile strength of weld for 4 mm thickness (Table 2), because as the thickness of plates increases the corresponding tensile strengths should reduce, as said in previous paragraph. Contrary to this the author have got tensile strength of 106.86 MPa for 5 mm thickness dissimilar plates, which is greater than 95 MPa for 4 mm thickness dissimilar plates as listed in Table 2. So one can intuitively conclude that

Table 2: Strength of welds of dissimilar materials FSW.

Sl. No	Thickness of plates (mm)	AS		RS		Tensile strength of FSW joint (MPa)	rpm	Welding speed (mm/min)	Reference
		Material	Tensile strength (MPa)	Material	Tensile strength (MPa)				
1	2	5052P-O	200	AZ31B-O	256	132	1000	300	[22]
2	3.25	AZ31B-H24	310	6063-T5	185	126	900 to 1400	117 to 202.8	[13]
3	4	6061-T6	310	AZ31B-H24	256	95	800	35	[24]
4	4	1060 Al	122.78	AZ31 Mg	274.66	82.4	315	30	[8]

for plates of thicknesses less than 5 mm or other thicknesses, this optimization procedure definitely yields higher values of tensile strength; i.e. higher than tensile strength of welds listed in Table 2, i.e. tensile strengths of 126 MPa and 132 MPa for 3.25 mm and 2 mm thickness plates respectively, because this EOP uses possible lowest rpm and medium V thus resulting in lowest thickness of IMs layers compared to higher rpm welds (as in Table 2); so one can conclude that, this experimental optimization procedure in FSW is especially suited for FSW of Al alloy to Mg alloy materials.

Every welding of plates of particular thickness can have its own highest strength, as said previously. One must not compare strengths of welds of different thicknesses plates. If one obtains weld for particular thickness of plate materials by following this optimization procedure he will get highest strength for the particular thickness of plates. In general as the thicknesses of plates decreases tensile strength of sound weld increases, irrespective of type of procedure or method used to obtain the sound weld, because as the thickness of plates reduces the volume of the IMs layer in weld volume decreases, resulting in increase in strength.

The unique characteristics of the optimization procedure are it yields highest strength of weld owing to use of lowest rpm generating lowest temperature level and use of medium welding speed, leading to a weld with least distortion and least residual stresses and least IMs thickness layer in weld volume compared to those of welds of high rpm. Welds with least distortion, least residual stress and least IMs thickness have high tensile strengths as reported here.

In the paper [38] the author nowhere reported about the IMs formed in the weld volume. But according to [13] formation of intermetallics (IMs) compounds are inevitable in the dissimilar Al–Mg weld joints under all conditions of welding. Strength of a chain is the strength of the weakest link in the chain. Since IMs have inevitably formed in the weld volume under all conditions of dissimilar Al to Mg alloy welding, IMs being brittle in nature and having very less strength, constitute the weakest part in the weld volume. So it can be concluded that the reported strength of 192 MPa by [38] is impossible to get in dissimilar Al to Mg alloy weld of plates thickness of 6 mm, and so it must be a fake result. Initially before FSW, Al and Mg alloy materials are in contact and also after FSW (under all conditions of welding) Al and Mg materials definitely will come into contact each other, so there is inevitable formation of IMs layers in the weld volume. In the paper [38] the authors, nowhere indicated or dealt about presence of IMs and thus leads to complete doubt about the data presented in the paper. Or another doubt is that the authors must have altered the data of results obtained by experiments. If you observe the above table, as the thickness of plates increases tensile strength decreases but, even though the authors used 6 mm plate, even then they have got 192 MPa high tensile strength, which is no way possible. Here the author has obtained a highest of 106.86 MPa, tensile strength for FSW between Al alloy and Mg alloy 5 mm thickness plates at possible lowest 300 rpm. So in the inevitable presence of IMs in weld volume the weld strength of dissimilar Al alloy to Mg alloy materials weld cannot be higher than 106.86 MPa (or around this value) for plates of thickness ≥ 5 mm as reported here. The contribution of lesser IMs layer thickness, to the strength of weld is more than the contribution of the tortuous nature of weld to the strength of the weld.

So the optimization procedure reported here yields possible highest strength welds for all thicknesses of plates since possible lowest rpm, and so lowest IMs thickness, as well as moderate tortuous welds, can be achieved. If this optimization procedure is assimilated for FSW of similar or dissimilar Al alloys, definitely one can get higher strength FSW joints due to evolution of high strength HAZ, than strength reported in literature e.g. [39].

One can find in FSW of similar materials literature (Mg alloys), FSwelds have been obtained at higher rpm (>600 rpm) i.e. at higher temperatures exhibiting higher tensile strengths. Tensile strengths were increased as the rpm increased. As the rpm increased temperature of the weld volume also increased and diffusion between the two similar material plates also increased which ensures effective bondage of the two materials at and around the interface of the two materials plates resulting in higher strength, owing to complete elimination of interface two surfaces and formation of continuous material body in place of interface. It is difficult to find higher rpm at which sound weld occurs giving highest tensile strength for similar materials (same or different Mg alloys). By EOP (experimental optimization procedure) one can determine lowest rpm at which sound weld occurs. Then one has to subject the sound welds to a constant high temperature (350–550°C for Mg alloys) for justified duration, and obtain the weld with highest tensile strength.

There are innumerable alloy combinations with innumerable hardness values; higher the hardness higher the rpm at which sound weld occurs for the given material combination. So, one has to repeat the trial and error methods, to fix the optimum parameters for different alloys, of the same thickness. So it becomes laborious procedure. But by EOP one can quickly arrive at optimum parameters irrespective of alloy material combination and thicknesses of materials to be FSWed.

Here in this dissimilar FSW highest strength of weld occurred for the sample having IO of 0.7 mm in RS. So one can conclude as follows; In AS, forward motion of the tool is more than that of in RS. So for similar materials FSW IO should be set in or towards AS. Material in AS is subjected to more deformation owing to more forward deformation plus less length of frictional or plastic deformation rubbing by tool; material in RS, less forward deformation plus long length of rubbing by tool. The net effect is almost equal plastic deformation for material in AS and for material in RS. In case of complete (in AS harder and in RS softer material) dissimilar materials welding, harder material has to be deformed for more length and more time, this is possible if and only if interface has kept in RS only.

This EOP yields sound weld at medium traverse speed and at possible lowest rpm. It is not possible to obtain sound similar or dissimilar welds at rpm > 500 rpm from this EOP. One can notice that, in order to obtain sound weld at higher rpm (>600 rpm), one has to adapt trial and error method (till now no one has obtained sound weld by following the EOP), so it is not an easy task to arrive to FSW parameters yielding sound weld at rpm > 600 rpm, but it is quite an easy task to obtain sound weld at lower rpm (<500 rpm) by following the EOP. This sound weld may not be having strength > that of sound weld obtained at higher rpms since there is no proper mixing of similar materials at the interfaces of the materials and so there will be no effective bondage between the two materials at the materials interface, owing to diffusion between the materials across both surfaces of interface, at low rpm, compared to that of weld at higher rpm. As explained previously, one can increase the strength of weld obtained by EOP by subjecting the weld to heat treatment i.e. one can determine practically the temperature to which the weld should be subjected and also its duration, so that resulting weld will have the highest strength.

Heat treatment above a particular temperature (Topt) will not give rise to higher values of tensile strengths, since at and around Topt, diffusion among the similar materials at interface completely eliminates interface or joint line remnant and produces almost homogeneous material, so any further increase in temperature above Topt will not give additional rise in strength. The author thinks that for FSW/FSP of similar precipitatable Al alloys, there is no necessity of heat treatment after FSW/FSP according to EOP developed here, because other than FSW heating, material may overage in HAZ region resulting in lower strength weld, but for FSW/FSP of Mg alloys heat treatment is a must since FSW of Mg alloy at higher rpm have greater strength compared to lower rpm welds.

3.9 Effect of intermediate material

Considering Exp. 2 or 3, intermediate metal Zn (or Cu) cannot be dissolved in Al alloy and Mg alloy materials owing to very less diffusion among the materials, owing to less rpm and so less temperature rise (around 350°C) in the weld volume; and also diffusion is very low because weld volume experiences less temperature level for only a few minutes of duration. Even at higher rpm welds (>1000 rpm) the temperature reached in the weld volume is around 475°C which is well below melting points of base metals or solidus temperature and also duration to which the materials will experience this temperature is of the order of a few minutes only. For diffusion to occur between metals not only the temperature is to be higher (>500°C) but also the metals must be maintained at the temperature for sufficiently long duration (hours to days) [47, 48]. But in FSW the temperature reached will be around 350 to 475°C [35] and also this will not last long for more than a few minutes. So owing to less temperature rise and insufficient diffusion, solid solutions could not be formed between and along the interfaces (Al, Zn and Mg, Zn). But IMs (if formed) will be formed at low temperatures or at low rpms (around 300 rpm); e.g. $Al_{12}Mg_{17}$ and Al_3Mg_2 IM compounds formed between Al alloy and Mg alloy at 300 rpm (Exp. 1).

One can say, there is very small scale diffusion occurring between layers of materials (between Al and Zn, and between Zn and Mg) in the weld volume because of low temperature and so low diffusion leading to neither formation of solid solution nor the formation of IMs at the materials interfaces. So these materials interfaces will become loosely held boundaries without any bonds in between them; so fracture occurs along these interfaces at almost zero stress.

Considering Exp. 4 and 5, any metal goes on softening at a constant rate (or flow stress of metal goes on decreases) from solid state (at room temp) to liquid state (melting point). The extent of the softening of the metal depends on the temperature level to which the metal is subjected to. Since weld volume (and the Ni) is subjected to lower temp (around 300–400°C at 305 rpm) the Ni foil is not softened enough (since Ni melting point is 1455°C) so that atoms of Ni would diffuse to nearby Al and Mg material and form IMs between Al and Mg. Since there is insufficient diffusion between Ni, Al and Ni, Mg there is no proper bonding and no proper IMs formation between Ni, Al and Ni, Mg; the interfaces between these become weak or have less strength leading to failure of weld in weld volume, at low tensile stress = 53 MPa. The lesser the material is softer (owing to material's lower temperature)

the less is the diffusion of atoms from the material to the nearby other materials. Tensile strength of weld with 0.1 mm Ni foil = 50 MPa < tensile strength of weld with 0.25 mm Ni foil = 53 MPa, owing to slightly more diffusion in higher thickness (0.25 mm) Ni foil.

In bare Al alloy to Mg alloy weld at 300 rpm there is sufficient diffusion between, enough softened materials Al alloy and Mg alloy (The melting points are 502–638°C and 605–630°C respectively compared to the melting point of Ni 1455°C) leading to formation of lowest thickness (enough thickness to withstand higher stresses) IMs $Al_{12}Mg_{17}$, Al_3Mg_2 giving rise to maximum tensile strength of 106.86 MPa. The weld between Al alloy and Mg alloy at lowest rpm (300 rpm) does not require any intermediate material since bare weld of Al alloy to Mg alloy itself has possible highest strength owing to formation of least thickness IMs. But for Al alloy to Mg alloy weld at higher rpm (>600 rpm), intermediate material such as Ni gives better strength. No other metals have melting points less than melting points of Al alloy and Mg alloy. So with regard to mutual diffusion and formation of IMs no metal will form IMs with Al alloy and Mg alloy having proper least thicknesses than IMs formed between Al alloy to Mg alloy at low rpm (305 rpm).

Analysis of results obtained by Woong [24] (see section 1, paragraph 7) by the author is as follows: the increase in tensile strength (=115 MPa) was owing to formation of lesser thickness layer of IM Ni_3Al compared to high thickness of IM layer $Al_{12}Mg_{17}$ owing to higher diffusion between Al alloy (melting point = 638°C) and Mg alloy (melting point = 630°C) since less diffusion occurred between Ni and Al materials owing to high melting point of Ni material. At 800 rpm, 35 mm/min parameters, higher temperature develops, leading to softening of materials (Al, Mg), involved in the welding. So there is considerable diffusion between Al alloy and Mg alloy materials; owing to higher diffusion at higher temperature, slightly higher thickness IM layer ($Al_{12}Mg_{17}$) forms yielding tensile strength of 95 MPa. When the Ni foil introduced and welding is performed at 800 rpm 35mm/min, Ni having high melting point (1455°C) softens less compared to Al alloy or Mg alloy at 800 rpm or at corresponding temperature. Diffusion from Ni to Al or Mg is less resulting in lesser thickness IM layer (Ni_3Al) formation in the weld volume compared to higher thickness IMs layer formed in weld volume of bare Al alloy to Mg alloy weld, and so higher strength resulted for the weld of Al alloy to Mg alloy keeping Ni as the intermediate material. IMs cannot be ductile in nature, so above said is the proper reason for increase of strength of weld with Ni as the intermediate material.

Phases shown in phase diagrams (PDs) can be obtained for equilibrium mixture of liquids of the materials involved. For solid to solid contacts one may not get these phases (shown in PDs). However for solid to solid diffusion 50–50% compositions of the solids in contact can be assumed. Strictly speaking only 50–50% mixture of liquid materials, give rise to phases in PDs, at 50–50% composition value.

3.9.1 Summary of the experiments

Authors experiments

Exp. 1

1. Thickness of Al alloy and Mg alloy plates = 5 mm
2. Rpm = 300
3. Traverse speed = 50 mm/min
4. Interface offset (IO) varied
5. Tensile strength of joint = 106.86 MPa [for sample with IM thickness (t) = 1.2 μm]; 95 MPa for 3 μm

Exp. 2

1. (1) to (4) same
2. Intermediate metal placed between Al alloy and Mg alloy of t = 0.25 mm and 0.1 mm
3. tensile strength of joints = 53 MPa (for 0.25 Ni) and 50 MPa (for 0.1 mm Ni)

Since melting point (mp) of Ni is 1450°C diffusion is lesser between Al and Ni and Mg, Ni so improper "t" of IM layer formed resulting in ten strength = 53 MPa. Fracture occurred in WN of samples.

Exp. 3

1. (1) to (4) same
2. Int Mat placed between Al alloy and Mg alloy of t = 0.25mm
3. This welded plate heat treated at 410°C for 10 min duration
4. Highest ten strength of this joint = 35 MPa and occurred at WN. The reason for less strength is owing to heat treatment higher t (>8 μm) of IM layers (NiAl, NiMg) formed in WN thus resulting in lesser strength (35 MPa) since higher the t of IM layer lower the ten strength.

Experiments of the Paper "[24]"

Materials used AA 6061-T6 and AZ31B-H24 of t = 4 mm.

Exp. 1.

800 rpm (quite a higher rpm for t = 4 mm), 35 mm/min (quite a larger heat input due to low traverse speed), so higher t of IM > 6 μm. Ten strength of this joint = 95 MPa.

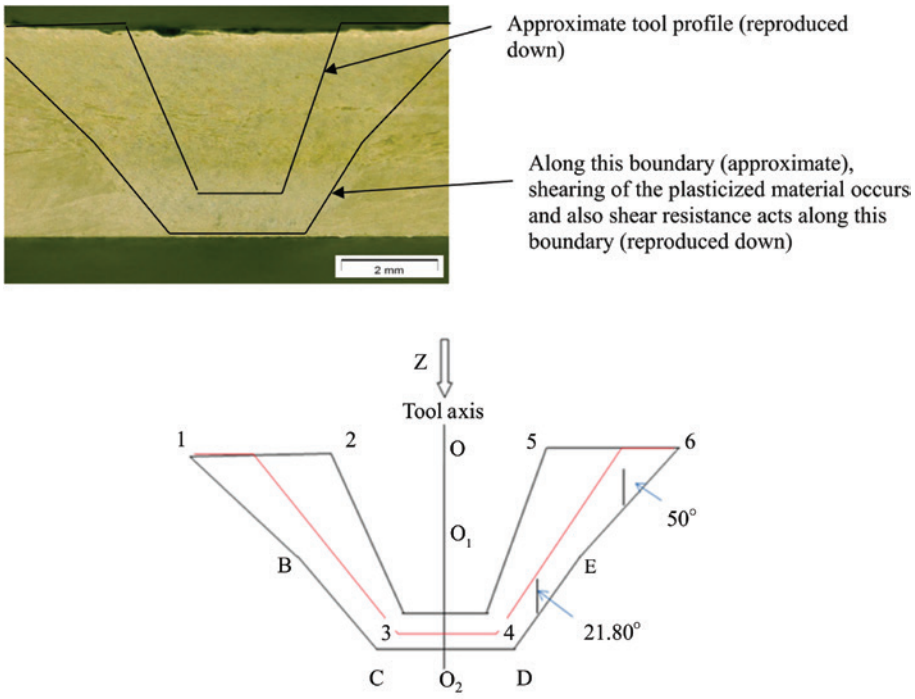

Figure 17: Tool profile and FSW volume cross section profile in friction stir welding of Mg alloy.

Exp. 2.
800 rpm and 35 mm/min with Int mat Ni = 0.5 mm t. Ten strength of this joint = 115 MPa due to improper formation of IM layers due to lesser diffusion (mp of Ni = 1450°C).

Exp. 3.
800 and 35, with Int mat Ni = 0.5 mm t with laser heating. Ten strength of this joint = 169 MPa; Ten strength is higher since lesser t (=4 mm) plates used and formation of even but lesser t (around 1 μm) of IM layer formation. Fracture occurred at HAZ.

3.10 Friction

As the seizure occurs between FSW tool and work piece, there will be no more relative motion between tool surface which is in contact with work piece material and work piece material immediately adjacent to FSW tool surface. So there is no more friction but there will be shear deformation between layers of work piece materials throughout the FSW volume, which contributes to temperature rise in and adjacent to weld nugget. Since material gets softened or plasticized in weld volume, total shear resistance (or equivalent frictional resistance) among the layers of material will be lesser compared to frictional resistance which occurs during initial plunging of tool and beginning of transverse motion of tool before seizure takes place. For Mg alloy plate defect free weld was obtained at 340 rev min^{-1} (Figure 1).

3.10.1 Equivalent coefficient of friction in bead on plate FSW of AZ31B-O Mg alloy

There is full seizure [49–53] between the tool (comprising shoulder and pin) and the material at the 3D surface (comprising shoulder surface and pin surface) on the tool. 1-2-3-4-5-6 (Figure 17) is the cross section of this 3D surface, which is also profile of the tool (Figure 17). Shearing of material takes place everywhere in the weld volume, i.e. between 1-2-3-4-5-6 and 1-B-C-O_2-D-E-6, the 3D profiles or surfaces; owing to this, shearing resistance occurs all over weld volume, around the tool pin. But if one assumes that the shearing resistance or equivalent frictional force (nearly similar to radius of gyration in mechanics), is restricted to or acts only on the weld volume outer profile 1-B-C-O_2-D-E-6 or on the middle profile (red line in Figure 17) or on the tool profile 1-2-3-4-5-6, then the equivalent coefficient of friction (μ_s) on the corresponding profiles can be determined as follows.

Consider the profile, 1-B-C-O_2-D-E-6. One can imagine a tool with shoulder diameter of the length "1-6" (from point 1 to point 6 in Figure 17) and pin of profile 1-B-C-O_2-D-E-6. One can consider resisting shear torque T_s with equivalent coefficient of friction μ_s on this surface or correctly, on 3D surface containing this profile.

The following are the formulae [54] for flat pivot and conical pivot under the assumption of uniform pressure.

$$T_s = [2/3]\mu_s Z R;\ R \text{ is radius; } Z \text{ is the Axial load.} \quad (1)$$

$$T_s = \left[2\mu_s Z\left(R_1^{\,3} - R_2^{\,3}\right)\right] / \left[3\left(\text{Sin}\alpha\right)\left(R_1^{\,2} - R_2^{\,2}\right)\right];$$
$$R_1, R_2 \text{ are radii; } \alpha \text{ is semi cone angle.} \quad (2)$$

Two conical surfaces are defined, first one which includes profiles 1-B and 6-E, projected area of this surface is A_1 and second, which includes BC, ED profiles, and projected area of this surface is A_2. Another surface which includes horizontal profile CD, having surface area A_3. The author measured the dimensions of lines ($O6 = 6.5$ mm; $O_1E = 3.5$ mm; $O_2D = 2.5$ mm; $OO_1 = 2.5$ mm $= O_1O_2$) by actual measurement on the physical sample shown in Figure 17, which was obtained for the following FSW parameters: rotational speed = 340 rev min^{-1}, welding speed = 60 mm min^{-1}.

So $A_1 = 94.24$ mm^2; $A_2 = 18.85$ mm^2; $A_3 = 19.634$ mm^2; $A_1 + A_2 + A_3 = 132.724$ mm^2; if the vertical load is Z ($=12.326 \times 10^3$ N, accessed from the archives of FSW machine computer system) on all surfaces together, load on each area is,

$$Z_1 = (94.24/132.724)\ Z = 8.752 \times 10^3 \text{ N};$$
$$Z_2 = (18.85/132.724)\ Z = 1.75 \times 10^3 \text{ N};$$
$$Z_3 = (19.634/132.724)\ Z = 1.823 \times 10^3 \text{ N}.$$

Let resisting shear torque be T_s with equivalent coefficient of friction μ_s.

Then from equation (2),

$$T_{s1} = [2 \times \mu_s \times 8.752 \times 10^3 (6.5^3 - 3.5^3)] / [3 \times (\sin 50)(6.5^2 - 3.5^2)]$$
$$= 58.837 \times 10^3\ \mu_s \text{N mm}$$

here (in the above equation), $R_1 = 6.5$ mm; $R_2 = 3.5$ mm; $Z_1 = 8.752 \times 10^3$ N; $\alpha = 50$;

$$T_{s2} = [2 \times \mu_s \times 1.75 \times 10^3 (3.5^3 - 2.5^3)] / [3 \times (\sin 21.80)(3.5^2 - 2.5^2)]$$
$$= 14.267 \times 10^3\ \mu_s \text{N mm};$$

here $R_1 = 3.5$ mm; $R_2 = 2.5$ mm; $Z_2 = 1.75 \times 10^3$ N; $\alpha = 21.80°$; and from equation (1),

$$T_{s3} = 2 \times \mu_s \times 1.823 \times 10^3 \times 2.5/3 = 3.0383 \times 10^3\ \mu_s \text{N mm}$$

here $R = 2.5$ mm; $Z_3 = 1.823 \times 10^3$ N.

Not only axial load Z along tool axis acts but also transverse load (F_t) along welding direction acts on tool. Owing to this transverse load ($F_t = 1.838 \times 10^3$ N, this data accessed from the archives of FSW machine computer system), acting on front ½ of the weld volume peripheral surface, additional resisting torque will be developed, this is T_{s4}.

$$T_{s4} = \mu_s \times 1.838 \times 10^3 \times 4 = 7.352 \times 10^3 \times \mu_s \text{ N mm};$$

where 4 mm is the average radius from Figure 4.

But the indicated torque accessed from the archives of FSW machine computer system $= 19.66 \times 10^3$ N mm; so

$$T_s = T_{s1} + T_{s2} + T_{s3} + T_{s4} = 19.66 \times 10^3.$$

Substituting values for T_{s1}, T_{s2}, T_{s3}, and T_{s4} from above calculations, one gets the equation for μ_s in canonical form as

$$83.4943 \times 10^3 \times \mu_s = 19.66 \times 10^3$$

$\mu_s = 0.234$ or 0.23. This is for the profile 1-B-C-O_2-D-E-6.

Considering red colored profile (Figure 17), by following the procedure mentioned earlier one can get, $\mu_s = 0.24$. Similarly considering tool profile 1-2-3-4-5-6 (Figure 17), one can get, $\mu_s = 0.25$.

If one divides the region between 1-2-3-4-5-6 layer and 1-B-C-O_2-D-E-6 layer into 10 layers, former being the 0th layer (where seizure occurs) and latter being the 10th layer. Then assuming equal, equivalent frictional force on each layer (excluding 0th layer but including 10th layer) with equal, equivalent μ_s on each layer; one can take 1/10 of vertical load, 1/10 of transverse load and 1/10 of torque for each layer. If one performs calculations as mentioned earlier for each layer, one can approximately determine equivalent μ_s on each layer. These μ_s values can then be used effectively in simulations, approaching actual conditions.

4 Conclusions

1. By experimental optimization procedure (EOP) optimum parameters for FSW between Al alloy and Mg alloy were determined and experiment conducted using these parameters resulted in not only sound weld but also highest strength weld for 5 mm thickness of the alloys plates.
2. One can arrive to optimum parameters by following the EOP in case of similar and dissimilar materials FSW, such as Al alloy and Mg alloy FSW.
3. It has observed that tensile sample having least thickness intermetallics (IMs) layer has highest strength compared to sample with larger thickness of

intermetallics layer and also it has observed that weld of lesser thickness plates have strength higher than welds of larger thickness plates.

4. It has observed that, Vickers hardness in WN i.e. on the region containing layer of IMs is considerably higher, which leads to emerge of new type of laminated composite materials.
5. It has observed that, it is the least thickness IMs layers in the weld are responsible for higher strength of weld not the ductility of the IMs formed owing to the insertion of intermediate material in the weld.
6. It has found that coefficient of friction is = 0.25, in case of bead on plate welding of Mg alloy.

Acknowledgments: The author is very thankful to IISc, Bangalore, India and DRDO, India (Grant No. DRDO/MME/SVK/0618) for sponsoring the project. The author would like to thank Prof. Satish V Kailas, Mechanical Dept, IISc, for his useful suggestions.

References

[1] Thomas WM, Nicholas ED, Needham JC, Church MG, Temple-Smith P, Dawes CJ. GB Patent Application No. 9125978.9. 1991.
[2] Liu G, Murr LE, Niou C-S, McCDluse JC, Vega FR. *Scripta Mater.* 1997, 37, 355–361.
[3] Dawes CJ, Thomas WM. *Weld J.* 1996, 75, 41–45.
[4] Thomas WM, Ncholas ED. *Mater. Des.* 1997, 18, 269–273.
[5] Su JQ, Nelson TW, Mishra R, Mahoney M. *Acta Mater.* 2003, 51, 713–729.
[6] Somasekharan AC, Murr LE. *Mater. Charact.* 2004, 52, 49–64.
[7] Sato YS, Seung CH, Michiuchi M, Kokawa H. *Scripta Mater.* 2004, 50, 1233–1236.
[8] Yan J, Xu Z, Li Z, Li L, Yang S. *Scripta Mater.* 2005, 53, 585–589.
[9] Hirano S, Okamoto K, Doi M, Okamura H, Inagaki M, Aono Y. *Q. J. Jpn. Weld. Society* 2003, 21, 539–545.
[10] Zettler R. *Adv. Eng. Mater.* 2006, 8, 415–421.
[11] Khodir SA, Shibayanagi T. *Mater. Trans. Jpn. Inst. Met.* 2007, 48, 2501–2505.
[12] Park SHC, Michiuchi M, Sato YS, Kokana H. In: *Proceedings of the International Welding/Joining Conference – Korea 2002*, Gyeongiu: KWS, 2002, 534.
[13] Venkateswaran P, Reynolds AP. *Mater. Sci. Eng. A* 2012, 545, 26–37.
[14] Venkateswaran P, Xu ZH, Li X, Reynolds AP. *J. Mater. Sci.* 2009, 44, 4140–4147.
[15] Kwon YJ, Shigematsu I, Saito N. *Mater. Lett.* 2008, 62, 3827–3829.
[16] Kostk A, Coelho RS, dos Santos J, Pyzalla AR. *Scripta Mater.* 2009, 60, 953–956.
[17] Li Y, Murr LE, McClure JC. *Scripta Mater.* 1999, 40, 1041–1046.
[18] Scialpi A, Giorgi MD, Filippis LACD, Nobile R, Panella FW. *Mater. Des.* 2008, 29, 928–936.
[19] Lee WB, Yeon YM, Jung SB. *Scripta Mater.* 2003, 49, 423–428.
[20] Watanbe T, Takayama H, Yanagisawa A. *J. Mater. Process. Technol.* 2006, 178, 342–349.
[21] Hua Z, Huiqiang W, Jihu H, Sanbao WN, Lin WU. *Rare Met.* 2007, 26, 158–162.
[22] Xu S, Deng X. *Acta Mater.* 2008, 56, 1326–1341.
[23] Bruck HA, Flower G, Gupta SK, Valentine TM. *Exp. Mech.* 2004, 44, 261–271.
[24] Chang WS, Rajesh SR, Chun CK, Kim HJ. *J. Mater. Sci. Technol.* 2011, 27, 199–204.
[25] Frigaard O, Grong O, Midling OT. *Metall. Mater. Trans. A* 2001, 32, 1189–1200.
[26] Mishra RS, Ma ZY. *Mater. Sci. Eng.* 2005, 50, 1–78.
[27] Song M, Kovacevic R. *Int. J. Mach. Tools Manuf.* 2003, 43, 605–615.
[28] Chen CM, Kovacevic R. *Int. J. Mach. Tools Manuf.* 2003, 43, 1319–1326.
[29] Schmidt HB, Huttel JH. *Scripta Mater.* 2008, 58, 332–337.
[30] Colligan KJ, Mishra RS. *Scripta Mater.* 2008, 58, 327–331.
[31] Beynon JH. *Tribol. Int.* 1998, 31, 73–77.
[32] Chen Z, Thomson PF. *Wear* 1996, 201, 221–232.
[33] Duffin FD, Bahrani AS. *Wear* 1973, 26, 53–74.
[34] Kumar K, Kalyan C, Kailas SV, Srivatsan TS. *Mater. Manuf. Process.* 2009, 24, 438–445.
[35] Mishra RS. *Friction Stir Welding*, ASM International: Materials Park, Ohio, 2007, 9, 44073–0002
[36] Prado RA, Murr LE, Soto KF, McCure JC. *Mat. Sci. Eng. A* 2002, 349, 155–165.
[37] Nadammal N, Kailasa SV, Suwas S. *Mater. Des.* 2015, 65, 127–138.
[38] Malarvizhi S, Balasubramanian V. *Mater. Des.* 2012, 40, 453–460.
[39] Kumar K, Kailas SV. *Sci. Technol. Weld. Join.* 2010, 15, 305–311.
[40] Yashan D, Tsang S, Johns WL, Doughty MW. *Weld. J.* 1987, 66, 27–37.
[41] Wang HY, Liu LM, Zhu ML, Wang H. *Sci. Technol. Weld. Join.* 2007, 12, 261–265.
[42] Chen YC, Nakata K. *Scripta Mater.* 2008, 58, 433–436.
[43] Kostk A, Coetha RS, dos Santos J, Pyzalla AR. *Scripta Mater.* 2009, 60, 953–956.
[44] Krishnan KN. *Mater. Sci. Eng. A* 2002, 327, 246–251.
[45] Kumar K, Kailas SV. *Mater. Sci. Eng. A* 2008, 485, 367–374.
[46] Gere T. *Mechanics of Materials*, 2nd edn., CBS Publishers: New Delhi, 2002.
[47] Callister WD, Jr. *Callister's Materials Science and Engineering*, Wiley India (P) Ltd: New Delhi, 2010.
[48] Abbaschian R, Abbaschian L, Reed Hill RE. *Principles of Physical Metallurgy*, SI edn., Cengage Learning India Private Limited: New Delhi, 2009.
[49] Somi Reddy A, Pramila Bai BN, Murthy KSS, Biwas SK. *Wear* 1995, 181–183, 658–667.
[50] Mosleh M, Saka N, Suh NP. *Wear* 2002, 252, 1–8.
[51] Chandrasekaran M, Batchelor AW, Loh NL. *Tribol. Int.* 2002, 35, 297–308.
[52] Krithivasan R, Khonsari MM. *Trans. ASME J. Tribol.* 2003, 125, 833–841.
[53] Pal AK. *Wear* 1973, 26, 261–272.
[54] Green WG. *Theory of Machines*, Blackie & Son Limited – London: Glasgow, 1958.